Runoff and nutrient loss from a water-repellent soil

Karin Muller, Karen Mason, Alfonso Gastelum Strozzi, Robert Simpson, Toshiko Komatsu, Ken Kawamoto, Brent Clothier, Alfonso Gastelum Strozzi

Preprint, published in Geoderma: Müller K, Mason K, Strozzi AG, Simpson R, Komatsu T, Kawamoto K, Clothier B 2018. Runoff and nutrient loss from a water-repellent soil. Geoderma 322: 28-37. https://doi.org/10.1016/j.geoderma.2018.02.019

Runoff and nutrient loss from a water-repellent soil

Karin Müller[1*], Karen Mason[2], Alfonso Gastelum Strozzi[3], Robert Simpson[2], Toshiko Komatsu[4], Ken Kawamoto[4], Brent Clothier[2]

[1]The New Zealand Institute for Plant & Food Research Limited (Plant & Food Research), Ruakura Research Campus Hamilton, New Zealand

[2]Plant & Food Research, Fitzherbert Science Centre, Palmerston North, New Zealand

[3]University of Mexico City, Mexico City, Mexico

[4]Saitama University, Saitama, Japan

Abstract

The effects of soil water repellency (SWR) on runoff and nutrient losses are difficult to isolate. Hydrophobic organic substances coating soil particles can severely delay water infiltration and enhance runoff. We used a portable run-on simulator to investigate the effect of SWR on runoff and nutrient loss. Intact soil slabs, 0.48 m long and 0.19 m wide, were collected from a severely water-repellent Andosol under pasture. One day before simulating 60-min long run-on events with an intensity of 60 mm h^{-1}, superphosphate was applied at a rate of 45 kg P ha^{-1}. The effects of SWR were quantified by comparing runoff volumes and nutrient losses from run-on events conducted with water and a fully wetting aqueous ethanol solution as run-on liquids. Further, through conducting multiple consecutive water run-on events with the same soil slab, the hypothesis, that SWR is lost through the washing off of hydrophobic materials, was tested. Finally, runoff dynamics were visualised by adding a dye to the run-on water. In the first run-on experiment, 88% of the water applied was captured as runoff, while no runoff was observed when aqueous ethanol was used as run-on liquid, providing strong evidence that SWR governed runoff generation from this Andosol. In consecutive water run-on experiments, approximately 23% of the applied P was recovered in the runoff from the first event, while the cumulative P loss over ten consecutive run-on events was around 30% of the applied P. This confirms that nutrient losses were associated with SWR and the occurrence of runoff. After ten consecutive run-on events, the persistence of both actual and potential SWR in areas of the slab that had been wetted were significantly ($p < 0.5$) reduced. But the persistence of potential SWR of the soil was still classified as severe, suggesting only minor losses of hydrophobic materials from the soil surface. The persistence of potential SWR and the degree of SWR of the dry areas remained more or less unchanged. In accordance with this, visualisation of the wetted areas showed that runoff occurred as rivulets guided by surface topography, rather than as sheet flow, with the wetted area increasing from approximately 20% of the slab in the first event to around one third of the total slab area in the final event. This pattern is reflected in the cumulative pattern of the P losses over the ten events. Consequently, we conclude that SWR should be considered as a factor in hydrological modelling and should be included in models to address appropriately the risk of surface water contamination by solutes exogenously applied to water-repellent soils.

Keywords: phosphorus; soil water repellency; hydrophobicity; infiltration; runoff simulation.

1. Introduction

The infiltration of water into water-repellent soils can be severely delayed when soil particles are coated with hydrophobic organic substances, which lower the wettability of the soil. This has implications for surface runoff and erosion, water storage and for plant growth. Many studies have suggested that surface runoff and overland flow increase with an increase in soil water repellency (SWR) (Ferreira et al., 2016; Gomi et al., 2008b; Keizer et al., 2005; Miyata et al., 2010; Valeron and Meixner, 2010). A majority of these studies focused on the impact of forest fires. Estimates of the increase in runoff and overland flow caused by SWR ranged from three (Burch et al., 1989) to 16 times (Leighton-Boyce et al., 2007). While many researchers have inferred that SWR enhances runoff and hence nutrient losses, the effect of SWR has only very rarely been isolated from other hydrological factors such as surface sealing and compaction (Keizer et al., 2005). Most attempts to quantify the effect of SWR on runoff have relied on indirect methods that attribute the increase of runoff to an increase in SWR (Gomi et al., 2008b; Leighton-Boyce et al., 2007). For example, runoff has been statistically correlated to SWR. One study measured the impact of SWR on runoff directly by comparing results when either water, or water plus a surfactant, was used in simulated rainfall experiments (Leighton-Boyce et al., 2007). It is a well-established method to assess the effect of SWR on infiltration by comparing the infiltration dynamics of water with those of a completely wetting liquid such as ethanol (Lamparter et al., 2010). Recently, we have adopted this method to study the effect of SWR on runoff (Jeyakumar et al., 2014).

Spatial variability of runoff connectivity and development of flow networks is directly related to rainfall intensity and soil infiltration capacity and is therefore also affected by antecedent soil moisture conditions (Cantón et al., 2011). Generally, runoff exhibits threshold behaviour such that the initiation of runoff requires a certain amount of rainfall. When the rainfall rate exceeds the rate of infiltration, excess water accumulates on the soil surface in depressions, forming puddles. Runoff starts once surface storage is filled and the puddles overflow (Horton, 1933). At a similar rainfall rate, the runoff rate depends on soil surface conditions including micro-topography, depressions, stone cover, water-repellent and surface hydraulic conditions (Gomi et al., 2008a). For example, a study analysing the temporal dynamics of runoff on forested hill slopes in Portugal found that runoff at times of strong to extreme SWR was significantly higher than when there was only slight, or no SWR (Pierson et al., 2009). The between-year variability in runoff and infiltration in soils with SWR was assessed in several burned and unburned sagebrush systems. The large variability indicated that the influence of SWR on runoff generation is quite variable, and its impact might be masked by short-term fluctuations in repellency (Pierson et al., 2008). As far as we know no studies have quantified runoff connectivity and the dynamic changes in runoff as influenced by SWR. To improve surface runoff modelling, better conceptualization of the underlying processes is necessary. Contreras et al. (2008) distinguished three runoff patterns for water-repellent soils. According to these authors all runoff hydrographs on repellent soils are characterized by the highest runoff rates at the beginning of an event. This assumes a water-repellent topsoil. The first runoff hydrograph type results from a rainfall rate exceeding the infiltration rate of the repellent topsoil layer. Runoff patterns then can be further differentiated depending on the existence of macropores and cracks or an underlying impermeable layer, which would lead to saturation-excess flow conditions. While SWR most often occurs in the topsoil, a water-repellent layer can also be sandwiched between wettable top and subsoil layers (Doerr et al., 2000). Thus, the suggested three runoff hydrograph patterns on repellent soils are not sufficient to capture the complexity of the response of water-repellent soils to rain.

Runoff studies are hampered by the unpredictability of runoff-generating rainfall events. The use of rainfall simulators is a reliable method for creating reproducible scenarios under semi-controlled conditions (Zhang et al., 1997). Major drawbacks associated with rainfall simulation studies are their small scale, the different characteristics of simulated rainfall compared with natural rainfall (Lascelles et al., 2000; Tossell et al., 1990), and high experimental costs. Rickson (2002) reviewed rainfall simulation techniques, highlighted issues related to the various approaches and techniques, and concluded that there is no ideal rainfall simulator. However, Neff (1979) concluded, 'we have no alternative' for investigating runoff processes. To avoid the discussion around the comparability of the heterogeneity and kinetic energy of natural and artificial rainfall, we decided to simulate inflow runoff (run-on) volumes to soil slabs instead of simulating artificial rainfall (Fabis et al., 1993) using our portable rainfall simulator (ROMA - RunOff Measurement Apparatus) (Jeyakumar et al., 2014). Run-on experiments allow to exclude the kinetic impact of raindrops on the soil surface and thus, to isolate the effect of SWR on water dynamics from other processes such as surface sealing. In contrast to others (e.g., Darboux et al., 2008), we use intact soil slabs to quantify the effect of SWR on runoff.

Our main objectives were (i) to quantify the effects of SWR on runoff and phosphorus (P) losses, (ii) to assess how SWR affects runoff and infiltration dynamics during successive events, and (iii) to investigate if rainfall leaches hydrophobic organic compounds from the soil, thereby requiring the input of new hydrophobic material to re-establish SWR following substantial rainfall.

2. Materials and methods

2.1. Collecting soil samples

Soil was collected from a severely water-repellent Pumice Soil (Andosol; FAO, 2006) under permanent pasture on a beef farm near Tihoi, New Zealand (-38.394959, 175.444809; GPS coordinates). On 20 December 2013, six intact topsoil slabs from a north-facing hillslope with an average slope of 16° were collected. On 27 November 2014, three additional intact topsoil slabs from the same hillslope were collected. All collected topsoil slabs were larger than the required size for the ROMA trays (0.2 x 0.5 m) and were wrapped in plastic to reduce the risk of damage and evaporative losses during transport to the laboratory. Four soil samples (0–0.05 m depth) were taken adjacent to each slab with a spade and immediately sieved (< 5 mm) to remove the thatch, a layer of organic matter accumulated around the base of the pastoral plants; the remaining soil (designated 'disturbed' soil sample) was placed in sealed plastic bags. In addition, intact soil cores (0.05 m diameter x 0-0.03 m) were collected close to the slabs in 2014. All slabs, cores and disturbed soil samples were stored at 4°C prior to conducting the experiments.

In November 2014, water infiltration rates into the topsoil were measured using tension disc infiltrometers at -70, -40, -20 and -10 mm tension in triplicate. Unsaturated hydraulic conductivity *K* was derived at each of these tensions as described by Reynolds and Elrick (2005). The infiltrometer results at a steady state, at each given tension were used to estimate the mean pore size weighted by flow, α, at this tension (Reynolds and Elrick, 1991). A large α indicated that the unsaturated flow was dominated by gravitational force, meaning that macropore flow dominated over matrix flow.

2.2. Determining physico-chemical soil properties

Approximately 100 g of each disturbed soil sample was passed through a 2-mm sieve. The gravimetric soil water content (GWC) and pH (in 1 M KCL) were measured using standard methodology (Blakemore et al., 1987). The pH meter was a Hanna HI 9812. Total soil organic carbon (SOC) and nitrogen content were analysed by the Dumas method for %C and %N using a Leco TruMac instrument (Blakemore et al., 1987). Hot water extractable carbon (HWC) was determined using the method developed by Ghani et al. (2003). Dissolved organic carbon (DOC) in the HWC extracts was determined by high temperature catalytic combustion using a Shimadzu TOC-V CSH total organic-carbon analyser (Ghani et al., 2003). For the second measurement campaign in 2015, subsamples for textural analysis were sieved to <4 mm, air-dried and dispersed using an ultrasonic vibrator before being separated into sand, silt and clay fractions using a sieving and settling process (Gee and Or, 2002). Bulk density was determined following standard procedures (Blakemore et al., 1987).

2.3. Conducting runoff experiments

Design and performance of the ROMA have been described in detail by Jeyakumar et al. (2014), where we conducted consecutive run-on events with water and a fully-wetting liquid on the same water-repellent soil slab. ROMA allows measuring volumes and rates of the applied run-on liquid running off the soil surface and draining below the soil slap depth. The set-up is shown in Fig. 1. In brief, a polycarbonate manifold with eight hypodermic needles is connected to a storage tank to simulate a constant run-on rate of 60 mm h-1. A constant pressure head is maintained by a floating switch controlled by a solenoid switch powered with a 12 V battery to ensure a steady run-on rate. The intact soil slab is fitted tightly onto a perforated tray adjusted to a slope of five degrees in order to simulate a hillslope situation. This tray accommodates drainage from the soil and retains the soil slab. Parallel to this perforated tray is a second tray, which collates the drainage. Runoff and drainage are collected in separate troughs (Fig. 1).

All field-moist soil slabs were trimmed to fit into the ROMA trays and air-dried in the laboratory at 21°C to a GWC between 0.25 and 0.3 g g-1. The persistence of actual SWR was measured on both the slabs and a subsample of the 5-mm sieved disturbed samples using water-droplet penetration tests ($WDPTT_{act}$; Doerr, 1998). A further subsample of approximately 80 g of the disturbed soil was oven dried at 65°C for 48 h, then placed in a sealed plastic bag to equilibrate at room temperature for 48 h prior to measuring the persistence of potential SWR ($WDPTT_{pot}$; Doerr, 1998), and the degree of SWR using the molarity of ethanol droplet test (MED, Roy and McGill (2002). In the MED test, the molarity of water and ethanol mixtures is varied repeatedly until droplets of the mixture infiltrate into the soil within 10 s. The molarity of this concentration (M) was used to calculate the contact angle following Roy and McGill (2002):

$$\gamma_c = 0.06105 - 0.01475 \ln(M + 0.5) \quad (1)$$

$$\cos\theta = \left(\frac{\gamma_c}{\gamma_w}\right)^{1/2} - 1, \quad (2)$$

Where γ_c is the surface tension of the ethanol solution and γ_w is the surface tension of water (N m^{-1}). The persistence of potential SWR and the degree of SWR are both measures of the potential of a soil to become hydrophobic when drying.

In contrast to the experimental set-up described by Jeyakumar et al. (2014), petroleum jelly and plastic liners were used between the soil slabs and side plates instead of expanding foam. Prior tests showed this to be more effective at preventing leakage along the sides of the slab. In addition, the bottom end of the slab was sealed with petroleum jelly to prevent wetting up due to runoff. Because of these changes, the new slab size was 0.19 m x 0.46 m, and the depth was kept at 0.05 m. The slope was set to five degrees, and pasture ground cover of the slabs was close to 100%. Thus, erosion was assumed to be negligible. All runoff experiments were conducted in triplicate. We conducted three sets of experiments each consisting of a number on run-on events: a run-on experiment with water followed by ethanol, and two run-on experiments consisting of consecutive water events.

2.3.1. Run-on experiment with water followed by ethanol, 2014

In the first set of ROMA experiments, the potential risk of fertilizer loss was quantified. Phosphorus, at a rate of 45 kg P ha^{-1}, was applied uniformly over the surface of each slab by distributing a mixture of superphosphate and acid-washed dry sand at a 1:5 ratio to the three replicates. The sand was used to facilitate the homogeneous application of the fertilizer. To isolate the effect of SWR from other potential hydrological parameters, we sequentially simulated run-on with two liquids (i) water and (ii) aqueous ethanol to the same soil slab, air-drying back to the initial GWC between the two run-on events. The aqueous ethanol (30% ethanol, v/v) was used as a reference full-wetting liquid with a smaller surface tension and specific density than water. Air-drying of the slabs back to the initial GWC, between run-on events was accomplished by monitoring the GWC of offcuts from the slabs, which received the same treatment as the slabs. The soil slabs were weighed before and after each run. To dry the slabs back to ± 1% of their initial weights, the weight obtained prior to the first run-on event was used as the reference. This method to assess the impact of SWR on runoff on different soil types has been successfully tested (Jeyakumar et al., 2014). Runoff and drainage volumes were collected, measured and sub-sampled over 5- or 10-min intervals during the 60-minute events with a run-on intensity of 60 mm h^{-1}. All subsamples were analysed for dissolved reactive phosphorus (DRP) and DOC. DRP was determined by Flow Injection Autoanalyzer following APHA's method 4500-P-G (2013) with a detection limit of 0.005 g m^{-}

^{3}. Results are presented as runoff and drainage coefficients (%), which were calculated as the sum of the entire runoff or drainage volume collected during an event divided by the total run-on volume applied per event.

2.3.2. Run-on experiment with consecutive water events, 2014

To test the hypothesis that water-repellent organic substances are washed out of repellent soil and need to be replenished for the soil to re-develop water repellency, we conducted ten consecutive 60-minute events with a run-on water rate of 60 mm h^{-1} on the same intact soil slab in triplicate. Between the consecutive events, the slabs were air-dried to their initial GWCs as described above. Superphosphate was applied at a rate of 45 kg P ha^{-1} as above. Runoff and drainage samples were collected over 5-min intervals during the initial five and the tenth events, and over 15-min intervals during the remaining events. The sample volumes were measured. Subsamples of all runoff and drainage samples were filtered through 0.45-µm cellulose acetate membrane filters and analysed for DRP and DOC as described above. After the tenth run-on event, SWR characteristics were measured at eight randomly selected points in the dry (water-repellent) and wetted (hydrophilic) areas following the standard methods outlined above. The dry and wet areas were distinguished visually. Slabs were then oven dried at 65°C for at least 8 days until constant weight was achieved and weighed to determine the dry weight of the soil.

2.3.3. Run-on experiment with consecutive water events, 2015

The ROMA was modified to increase water run-on uniformity by oscillating the polycarbonate tube delivering the water. It had a horizontal range of 15 mm at a constant rate of 40 oscillations min^{-1} across the top of a slab (motor, PITMANN GM 8712, Harleysville, PA). The experimental design was also modified to improve our understanding of the interactions between SWR, runoff and the processes observed. To visualise runoff dynamics and wetting-up patterns of the soil, and to investigate if water-repellent conditions and runoff/drainage patterns could be reproduced after heavy rainfall events, Food Colour FCF Brilliant Blue (Narmada Colours Private Ltd., Gujarat, India) was added to the run-on water at a rate of 83 mg L^{-1} applied to three replicates. As the dye was used only to trace flow paths, its potential adsorption to soil particles was irrelevant (Flury and Flühler, 1995). We collected and measured runoff and drainage volumes over 10-min intervals. The runoff and drainage samples of each runoff event were bulked into a single runoff volume, and a single drainage sample per event. These were analysed for DOC as described above. In 2015, the water run-on events were repeated until the average runoff coefficient during the 60-min event was < 10% and the drainage coefficient was > 70%. Drying of the soil slabs followed the protocol presented in 2.3.2. The persistence of actual SWR was measured at five randomly selected points in the dry, and wetted (stained) areas, immediately before each run.

Runoff dynamics were visualised via staining the run-on water with brilliant blue. Images of the slabs were captured during the run-on events using a tripod-mounted Nikon D700 camera (Nikon Imaging Japan Inc., Tokyo, Japan) with a Nikon 50.0 mm f/2.8 lens. The digital camera was fitted with a 36.0 mm x 23.9 mm FX CMOS sensor with approximately 12.1 million effective pixels. The camera was used in its manual mode where shutter speed, focus and aperture were manually selected. The optimal settings, a 0.5-s exposure time, ISO 800 mode, F-stop 18, 50-mm focal length, and a distance of 0.68 m from the top of the slab were determined prior to starting the events and kept constant. The image size was 4256 x 2832 pixels, with a pixel density of 1.41 MP cm^{-2}. Photographs were taken of the slab prior to each event and at 5, 10 and every 10 min thereafter for the duration of each event. A metal grid with 32 squares (47.5 x 49 mm i.d. of the squares) was mounted above the slabs and a grey colour card was incorporated into each image for analysing any potential optical distortion.

2.4. Image Analysis

The dynamics of the flow-path development on the soil surface over time were visualised and quantified by the sequence of the photographs taken for every run-on event. These provided information on the temporal and spatial patterns of development of the active surface-runoff pathways during a single run-on event, and over a sequence of run-on events performed on the same soil slab. The stained area can be understood as an upper limit of the area involved in runoff.

For each soil slab, a stack of images was defined using the photographs taken during all run-on events conducted per slab. The stack of images from each slab were aligned with an ImageJ Java plugin (https://imagej.net/Linear_Stack_Alignment_with_SIFT) implementing the Scale Invariant Feature Transform (SIFT) method (Lowe, 2004). The alignment was done to correct for possible changes in the camera position during photograph acquisition. The aligned stack of images allowed monitoring changes in the pixels' hue and saturation values due to changing dye concentrations over time.

All pixels of all these aligned images per slab were used and segmented into stained and unstained pixels, using a fuzzy c-means algorithm (Bezdec, 1981). The method provided a set of values, not a single thresholding value, for the hue, the saturation and the value of the HSV colour space that were used to classify each pixel as stained or non-stained. The segmentation provided information on the development of the total number of stained pixels for each soil slab during a run-on event, which was expressed as the active runoff area of the total slab area. Segmentation was performed in a solution developed using MATLAB (The MathWorks Inc., 2017). To analyse how the dye moved across the slab, the reference metal grid was used to divide each slab into 32 regions. These regions were used to quantify the number of stained pixels per region, and to evaluate the runoff pattern across a slab.

2.5. Statistical analysis

All data were analysed using an analysis of variance (ANOVA) with a 5% level of significance. Statistical analyses were carried out using the statistical package GenStat (version 14.2.0.6297, VSN International Ltd). Figures were prepared using SigmaPlot version 12.5.

3. Results and discussion

3.1. Soil properties

The topsoil of the Andosol was characterized by high total-carbon contents between 10.5 and 15.1% (Table 1). The variability might have been related to the local disturbance of vegetation as well as the heterogeneous spread of dung and urine by grazing livestock, which was also supported by the large variability of the HWC concentrations. The top 0.05 m of the soil was composed of 7% clay, 37% silt and 56% sand, and had a bulk density of 0.742 ± 0.026 kg m^{-3}. The pH of the soil was consistently low. The persistence of actual and potential SWR ($WDPT_{act}$ and $WDPT_{pot}$) for all slabs used in this study can be classified as severely (600 s – 1 h), and extremely persistent (>1 h) respectively (Dekker and Jungerius, 1990). All soils had the potential to develop hydrophobic conditions, as reflected in their contact angles (CA) of well above 90^{o} (Table 1). The unsaturated hydraulic conductivities close-to-saturation measured in November 2014 were 0.2, 0.3, 1.1 and 3.3 mm h^{-1} at -70, -40, -20 and -10 mm, with coefficients of variation between 30 and 70%. These are lower than expected *K*-values for Andosols, soils that are known for their rapid water infiltration and conductivities (Arnalds, 2008). This could partly be explained by the water-repellent state of the soil. The persistence of actual SWR determined close to the infiltrometers was between 2 and 135 s, with an average of 19 s, which classifies the SWR status of the soil as slightly persistent (Dekker and Jungerius, 1990). For the two lower tensions, the flow-weighted mean pore size, α, was larger or very close to 0.3 mm, the threshold for macropores according to Jarvis (2007), indicating that macropore flow could have been an important flow path in this soil (Burch et al., 1989). The trend was for higher K-values at the sites with slightly higher repellency, but the measurements were too few in number to draw any conclusions about the effect of repellency on macropore flow.

3.2. Effects of repellency on runoff and P losses

Generally, research investigating the effect of SWR on runoff is inferred from observations on the coincidence of the occurrence of SWR and runoff in the field throughout different seasons (Ruiz-Sinoga et al., 2010; Shakesby et al., 2000). Our experiments with intact soil slabs under controlled laboratory conditions allowed us to isolate and measure the effects of SWR on runoff using soil slabs that were extracted at the same time of the year (Jeyakumar et al., 2014). It needs to be stressed that these experiments are not representing field conditions of rainfall events. The main purpose of the run-on experiments was to analyse the effect of SWR on runoff and P-losses via runoff while excluding other hydrological factors such as surface sealing through the kinetic impact of rainfall. The initial average SWR characteristics of the slabs used in the first runoff experiments classified the soil as extremely hydrophobic (Table 1).

While no runoff occurred in the ethanol events, which reflects the response of the soil to rainfall under hydrophilic conditions, average runoff coefficients of the associated water events were very high, averaging 88 ± 8% for three slabs over the 60-min events (Figs 2a and c). This provided strong evidence that SWR governed runoff. In accordance with this, the short lag time of less than 5 min for runoff initiation also pointed to infiltration excess as the runoff generating process (Fig. 2a). Consistent with these results are the very low unsaturated hydraulic conductivities close to saturation (<5 mm h^{-1}). Interestingly, the average runoff coefficient stayed very high throughout the 60-min runoff run-on event. This agrees with the high initial degree and persistence of SWR, but is inconsistent with the soil carbon content. The runoff response observed is similar to that of an Organic Soil with 22% OC (Jeyakumar et al., 2014), while the Andosol used in this study had half this OC content (Table 1). This highlights that the nature, not only the quantity, of OC is relevant for the persistence of SWR (Horne and McIntosh, 2000).

Drainage started after approximately 30 min, and stayed below 10% of the water rate applied (Fig. 2a). After drying the soils to their initial GWCs, the average $WDPT_{act}$ and $WDPT_{pot}$ were 6,267 ± 2,135 s and 9,800 ± 1,470 s, respectively, while the degree of SWR (CA) was 102.5 ± 0.6°. This underscores that the water-repellent status of the soil had not changed significantly ($p > 0.05$) during the initial water runoff event. Subsequently, as described above, ROMA run-on events were repeated with ethanol and no runoff occurred (Fig. 2c). Our experiment confirms the connection between SWR and the occurrence of runoff, a relationship that has been mostly inferred but not measured, until now (Doerr and Moody, 2004).

Losses of the P applied to a water-repellent topsoil were directly quantified. DRP concentrations in runoff samples were highest in the first 5 minutes of the 60-minute experiment, and decreased exponentially with time (Fig. 2b). In total, 18 ± 6.9% and 1.5 ± 0.1% of the applied P were lost as DRP in runoff and drainage, respectively. Losses were comparatively low considering that the average runoff coefficient exceeded 80%, and that risks for P losses via runoff are highest for recently applied fertilizers (Hart et al., 2004). We restricted the runoff analysis to DRP because in our run-on experiments erosion, and thus particulate P transport, were considered to be negligible. No sediment was visible in the runoff samples. In addition, Hart et al. (2004) highlighted in their review of previous research on P runoff from agricultural land that DRP losses are the dominant P fraction lost via runoff in drier years and in summer and autumn. Solute extraction from water-repellent soils, and losses in runoff, are restricted to the solutes available in the active runoff areas. In accordance with our findings, Jeyakumar et al. (2014), who used an inert tracer in their ROMA experiments, reported tracer losses between 8 and 13% of the applied amounts in surface runoff, in spite of runoff coefficients larger than 50%.

3.3. Switching between hydrophobic and hydrophilic soil conditions

The three soil slabs used for the consecutive run-on events with water in 2014 were extremely hydrophobic (Table 1). As expected from our previous experiment and the SWR status of the soil, runoff was observed for all intact soil slabs in the first event. In the sequence of run-on events with water, the runoff coefficient dropped from the first to the third event, but stayed relatively constant within each of these three events. During later run-on events, the runoff coefficient decreased exponentially with time over the event, with R^2 values ranging between 0.94 and 0.99 (Fig. 3a). But even after ten consecutive events, runoff still occurred during the first 30 min of the events, albeit at rapidly decreasing rates. Resulting average runoff coefficients were 89 and 12% for events 1 and 10, respectively (Table 2). Drainage mirrored these runoff patterns (Fig. 3b), with average drainage coefficients of 5 and 54% in run-on events 1 and 10, respectively (Table 2). The increasing infiltration and drainage rates during later events suggest a breakdown of SWR, or wash-out/ wash-off of hydrophobic organic substances. The repeated wetting/ drying cycles were not expected to significantly change the soil's structure because the pastoral free-draining and well-structured soil had a low clay content and a low bulk density (Table 1), and, in addition, the slabs were dried under ambient conditions.

After ten cycles of simulated run-on and drying, water contents and repellency characteristics were separately determined for the dry and wet areas of the three slabs (Table 3). The wet areas of the slab were saturated. As expected, these areas were hydrophilic after 10 run-on events. DOC was washed off the soil slabs via runoff (Fig. 4) or leached via drainage (data not shown); this could have been linked to washing out/washing off of soluble water-repellent organic compounds. While the load was highest for the first run-on event, the change in the pattern of the runoff coefficients observed in event 4 (Fig. 3a) was not correlated to DOC loads, suggesting that the DOC washed off, or out, was not necessarily hydrophobic. While the persistence of potential repellency for the wet areas was reduced, it was still classified as severe. Of interest, the degree of repellency had not changed significantly ($p < 0.05$) for the wet areas (Table 3). This highlights that the soil still had the potential to develop repellency upon drying, and therefore challenges the hypothesis that all water-repellent material was washed out, or off.

In contrast to the wet areas, the dry areas of the slab had a higher persistence of actual SWR than the initial slab, which might be related to selective drying of the soil during air-drying. Selective drying was confirmed by the difference between the initial soil water content and the water content of the dry areas after 10 events. The latter was on average 0.141 ± 0.017 g g^{-1} compared with the average initial water content of the entire slab of 0.372 ± 0.043 g g^{-1}. The dependence of SWR on soil water content is well known (de Jonge et al., 1999; Regalado and Ritter, 2005; Wijewardana et al., 2016). Seasonal variations of hydrophobic and hydrophilic soil conditions based on measurements of the persistence of actual SWR can be confounded by differences in soil water contents (Dekker et al., 2001; Müller et al., 2014), as also described here. The persistence of potential SWR and the degree of SWR remained unchanged within experimental error in the dry areas after the 10 run-on events (Table 3). Over ten consecutive run-on events, on average 29% of applied P was lost as DRP in runoff, of which 79% was lost in the first event (Table 2). This suggests relatively stable, active runoff pathways over the ten events. To analyse runoff patterns of water-repellent soils over a sequence of run-on events, we stained the run-on water for the next set of experiments.

3.4. Recurring active runoff areas

All three soil slabs collected in 2015 were extremely hydrophobic (Table 1). All slabs responded to the simulated run-on with runoff during all events. During the fourth event, the average runoff coefficient was below 10% for all slabs, with the exception of one slab. With this slab, five events had to be performed to fulfil the pre-defined experimental cut-off criteria (average runoff coefficient <10%; drainage coefficient >70%). In the sequence of water events, the runoff coefficient averaged over an event dropped from 90 ± 7.6% in the first event, to 7 ± 4.2% in the fourth event, while the average drainage coefficient increased from 5.5 ± 7.6% to 71.1 ± 24.3%, thus mirroring the runoff pattern. Similar to the 2014 experiments, later runoff responses, i.e. the third and fourth events, were described with an exponential model with R^2 values of 0.91 and 0.93. The water retained in the slab was on average 4.5 ± 4.1%, 12.6 ± 8.5%, 16.1 ± 9.1%, 22 ± 11.9% and 21.4% of the applied run-on water for the four, and for the last slab's five events, respectively (Fig. 5).
Staining the run-on water allowed visualisation of runoff flow pathways and identification of the slab areas where runoff occurred. These areas were referred to as stained or active runoff areas. The active runoff area increased during the first event on average from 12 ± 3%

measured after the first 5 min, to 30 ± 5% of the total surface area of a slab after 60 min. This increase was significant ($p < 0.05$) (Fig. 6). Runoff was triggered as an infiltration-excess runoff governed by SWR. However, the initiation of runoff via infiltration-excess was also dependent on 'filling and spilling' of depressions, and thus the micro-topography of the slabs. The increasing water depth during an event connected more and more filled depressions to the active runoff area through spilling and merging. This was reflected by the increasing active runoff area during an event. Generally, the number of stained pixels per region of a slab increased throughout each event (data not shown), and from event to event (Fig. 7). The final active runoff area at the end of the four events conducted was only significantly ($p < 0.05$) different for run 1 with 22 ± 4%, compared with runs 2, 3 and 4 with 31 ± 4%, 33 ± 5% and 33 ± 4%, respectively (Figs 6 and 7). The active runoff area for all slabs never exceeded a third of the entire slab area, which would have been driven by interactions between surface roughness and persistence of SWR (Gomi et al., 2008a). These results highlight that runoff from water-repellent soils does not occur as homogeneous sheet flow, but in rivulets, which was supported by the visualization of the flow patterns in the different slab regions shown in Figure 7. However, it needs to be pointed out that similar studies with the same soil under unconfined conditions need to be carried out to confirm that these percentages were not caused by boundary effects resulting from the experimental set-up. We postulate that the observed phenomenon of recurring active runoff areas for a water-repellent soil is comparable to the vertical re-wetting of flow pathways in water-repellent soils during a sequence of rainfall events (Ritsema, 1997). In the case of vertical flow, hydrophobic compounds are leached from pores along finger flow pathways, which then develop into permanent flow pathways (Ritsema et al., 1998). Here, in the case of runoff, the persistence of SWR can be broken down through water ponding in depressions, which might result in a reconfiguration, leaching or washing out/off of hydrophobic compounds (Urbanek et al., 2014). The hydrologic connectivity of the active runoff areas enhances the breakdown of SWR by the re-distribution of water. Contact and lateral diffusion from wetted into water-repellent areas (Doerr and Thomas, 2000) and capillary rise from saturated subsoil layers upon drying (Shakesby et al., 2000) can take place. The persistence of SWR quantifies by how much infiltration is delayed. A higher persistence of repellency causes longer ponding, and/or earlier threshold flow depending on the micro-topography, underscoring the importance of persistence of SWR for hydrological effects of SWR (Doerr and Moody, 2004).

To support our hypothesis that hydrophobic material is leached during rainfall events, before each event, $WDPT_{act}$ was measured separately for the stained and unstained slab areas on the air-dried slabs. For all slabs, and all events, the persistence of SWR was consistently lower in the stained than in the unstained areas. However, it never reached a fully wettable state. Average values for the stained areas were 107 ± 30 s, 122 ± 39 s, 314 ± 84 s and 107 ± 13 s for the run-on events 2, 3, 4 and 5, respectively, which can all be classified as strongly persistent repellent (60 – 600 s). The variability of the measurements was large. The active runoff areas were characterized by a significantly ($p < 0.05$) lower persistence of SWR than the dry areas. The latter were all classified as persistent and severely repellent (600 – 3600 s). After 4 to 5 events, the run-on water was effectively channelled within a few minutes into the active runoff areas, with lower persistence of SWR. Here the water filled the depressions and eventually infiltrated, reducing the total runoff volumes to less than 10% of the total run-on volume. Accordingly, the active runoff area was positively ($p < 0.001$) correlated to the drainage coefficient ($R = 67.92$) and negatively ($p < 0.001$) correlated to the runoff coefficient ($R = -88.29$). All parameters were measured at the seven sampling times during each event.

The average total DOC load per experiment in the runoff generally decreased over the sequence of run-on events, but the average DOC load in drainage increased (Fig. 8). No correlation was found between the DOC loads and the SWR characteristics determined before each event (data not shown).

4. Conclusions

We have identified SWR as a factor leading to runoff and P losses. Persistence of actual SWR was reflected in the high runoff coefficient throughout one-hour run-on events. The breakdown of repellency during repeated runoff events could not be linked directly to the wash-out of hydrophobic material. About 20% of the surface-applied P-fertiliser was washed off in the runoff induced by SWR, showing that the risk of solute losses from water-repellent soils was somewhat restricted to the active runoff area in our experiments. This was further highlighted by the fact that about 80% of the losses over 10 and four sequential events occurred in the first event, and the relatively small growth of the active runoff area after the first event. In addition, the recurrence of active runoff areas in this water-repellent soil was observed.

Further experiments are required in which micro-topography is measured in parallel with SWR. Connectivity models considering micro-topography and the patchiness of the persistence of SWR may provide a way to model runoff from water-repellent soils successfully, and then link point and plot-scale measurements to impacts at larger spatial scales. Field experiments are required to assess on larger scales the relevance of the processes analysed in the lab. In summary, we have shown that SWR should be considered as an important factor in hydrological modelling, and should be included in models to address appropriately this increased risk of surface water contamination by solutes exogenously applied to water-repellent soils.

Acknowledgements

The project was funded through a bilateral New Zealand Ministry of Business, Innovation and Employment (MBIE)/ Japan Society for the Promotion of Science (JSPS) project (C11X1210). Funding from the European RISE-project PROTINUS allowed us to analyse the images acquired during the runoff experiments conducted in 2015. We thank Mike and Sharon Barton for access to their farm and for their ongoing interest and support of our research. Thanks are due also to Tony Corbett, who helped with the image acquisition. We thank Charlotte Robinson and Jade Gribben for their assistance with conducting the runoff experiments.

Figure captions

Figure 1: A schematic diagram of the run-off measurement apparatus (RunOff Measurement Apparatus; ROMA). Reproduced from Jeyakumar et al. (2014).

Figure 2: (a) Surface runoff and drainage coefficients (runoff or drainage volume as a percentage of run-on volume) in laboratory run-on events with water. (b) Dissolved reactive phosphorus (DRP) concentrations in runoff. (c) Runoff and drainage coefficients in run-on events with 30% ethanol on the same soil slabs. All results are averages of 10-min intervals over the 60-min run-on events for three slabs. Bars represent standard deviations of the means.

Figure 3: (a) Runoff and (b) drainage coefficients (runoff or drainage volume as a percentage of run-on volume) in a sequence of ten events conducted with the same soil slab and air-drying back to its initial gravimetric soil water content after each run-on event. All results are the averages over three slabs. For the sake of clarity, no variability measures are presented.

Figure 4: Dissolved organic carbon (DOC) loads in runoff from ten consecutive run-on events on the same soil slab with air-drying between the run-on events. All results are averaged over three experiments. Bars represent standard deviations of the means.

Figure 5: The water balance for the five consecutive water runoff events conducted in triplicate. The average of the run-on water recovered as runoff, drainage or water retained in each of the soil slabs is presented.

Figure 6: Development of the active surface runoff areas over time for the four to five consecutive water runoff events conducted, here shown for one of the three soil slabs.

Figure 7: Segmented images (left) and number of stained pixels per segment of the reference grid determined at the end of each run-on event (right). Number of images each pixel was stained during a run-on event, e.g., 14 means that a pixel was stained from the first to the last image taken (left). The size of stained area per segment of the reference grid was determined at the end of each run-on event. The size of the dots at each grid coordinate is proportional to the number of stained pixels per segment (right). Both results are shown for one of the three soil slabs and the four consecutive runs (top to bottom).

Figure 8: Average total dissolved organic carbon (DOC) load over the sequence of four water run-on events. The bars are the averaged results for three soil slabs. The error bars represent the standard deviation of the means.

Tables

Table 1: Average basic soil properties including total organic carbon (TOC), total nitrogen (TN) and hot water carbon (HWC) as well as the persistence of actual and potential SWR ($WDPT_{act}$, $WDPT_{pot}$), and degree of soil water repellency (contact angle, CA) for disturbed soil samples collected adjacent to the respective intact soil slabs. Figures are averages ± standard deviations of three replicates.

Lab ID	TOC (%)	TON (%)	C:N (-)	pH (-)	HWC (µg g^{-1})	$WDPT_{act}$ (min)	CA (°)	$WDPT_{pot}$ (min)
Slabs 2014 – water & ethanol experiments								
7	10.86	0.91	11.96	4.3	2703	110 ±48	101.2 ±0.7	155 ±43
8	14.53	1.20	12.10	4.5	1256	30 ±4	100.7 ±1.3	65 ±18
9	10.50	0.88	11.89	4.6	1450	180 ±0	102.1 ±1.0	180 ±0
Slabs 2014 – consecutive water experiments								
3	15.07	1.23	12.27	4.4	1424	24 ±3	100.7 ±0.5	88 ±42
4	12.61	1.10	12.61	4.2	2142	13 ±3	100.2 ±0.0	130 ±35
6	11.33	0.93	12.18	4.3	3024	13 ±0	101.2 ±0.3	130 ±17
Slabs 2015 – consecutive water experiments								
1	13.1	1.09	12.01	4.3	4380	18 ±0	101.7 ±1.0	95 ±17
2	11.5	0.95	12.19	4.5	4105	18 ±0	100.2 ± 1.0	62 ±12
3	14.9	1.23	12.19	4.6	5679	68 ±12	102.5 ±1.0	145 ±17

Table 2: Average runoff and drainage coefficients, and dissolved reactive phosphorus (DRP) losses in run-on events 1, 10 and totalled over the ten consecutive run-on events. Figures are averages ± standard deviations of three soil slabs.

	Event 1	Event 10	Over 10 events
Mean runoff coefficient (%)	89 ±7	12 ±16	
Total DRP in runoff (%)	22.9 ±2.8	0.3 ±0	29 ±2.5
Mean drainage coefficient (%)	5 ±6	54 ±14	
Total DRP in drainage (%)	0.8 ±0.5	0 ±0	2.7 ±2.3
Total DRP loss (%)	**23.7**	**0.3**	**31.5**

Table 3: Average water content and soil water repellency (SWR) characteristics before the initial and after the tenth water run-on event. After the tenth event, hydrophilic (active runoff rivulets) and hydrophobic (dry) areas of the soil slabs were analysed separately. Classification of the persistence of SWR: Class 0, wettable; Class 1, slightly persistent SWR (5–60 s); Class 2, strongly persistent SWR (60–600 s); Class 3, severely persistent SWR (600 s–1 h); Class 4, extremely persistent SWR (>1 h) (Dekker and Jungerius, 1990). Results are averages ± standard deviations of the mean of three slabs; measurements were replicated eight times in each area.

Event number	**0**	**10 – hydrophilic areas**	**10 – hydrophobic areas**
Water content (g g^{-1})	0.372 ±0.043	0.899 ±0.011	0.141 ±0.017
$WDPT_{act}$ (s)	983 ±404	0 ±0	4800 ±2078
$WDPT_{pot}$ (s)	7800 ±1859	3100 ±2058	7100 ±2194
MED (°)	100.87 ±0.57	100.43 ±1.09	101.2 ±0

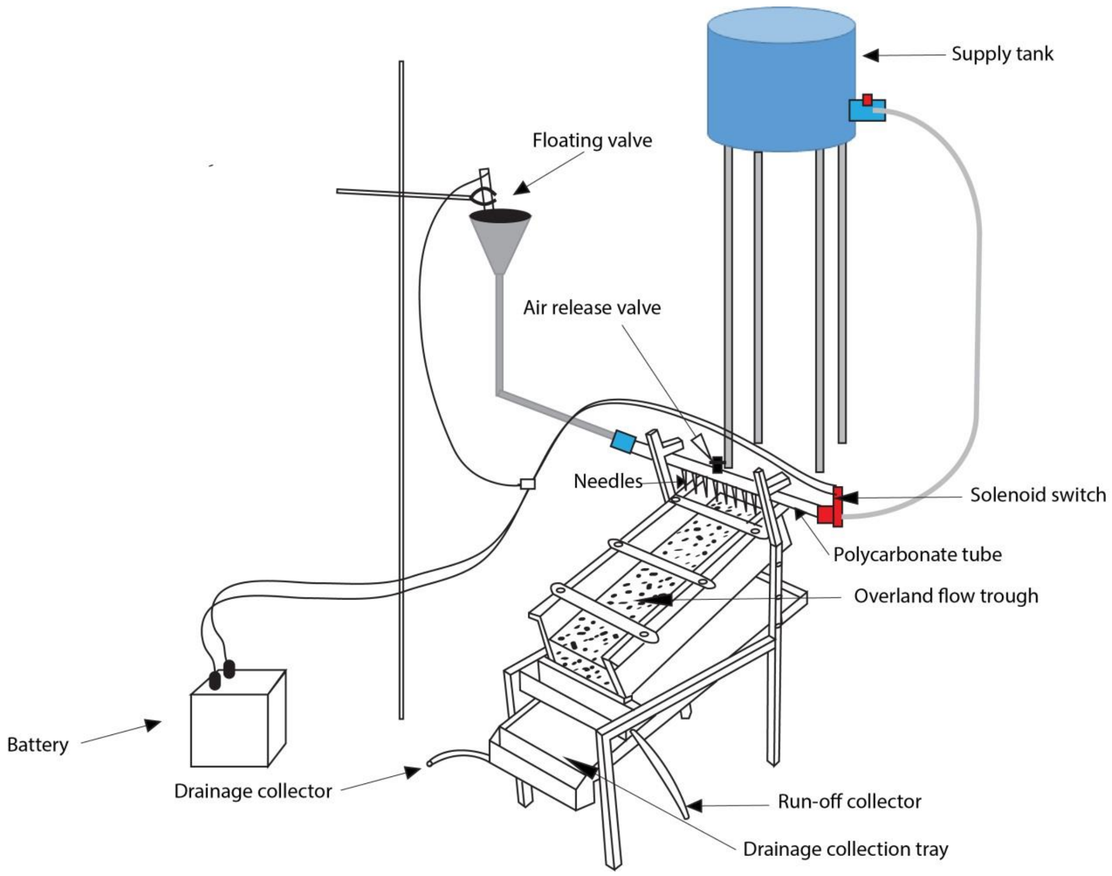
Supply tank
Floating valve
Air release valve
Needles
Solenoid switch
Polycarbonate tube
Overland flow trough
Battery
Drainage collector
Run-off collector
Drainage collection tray

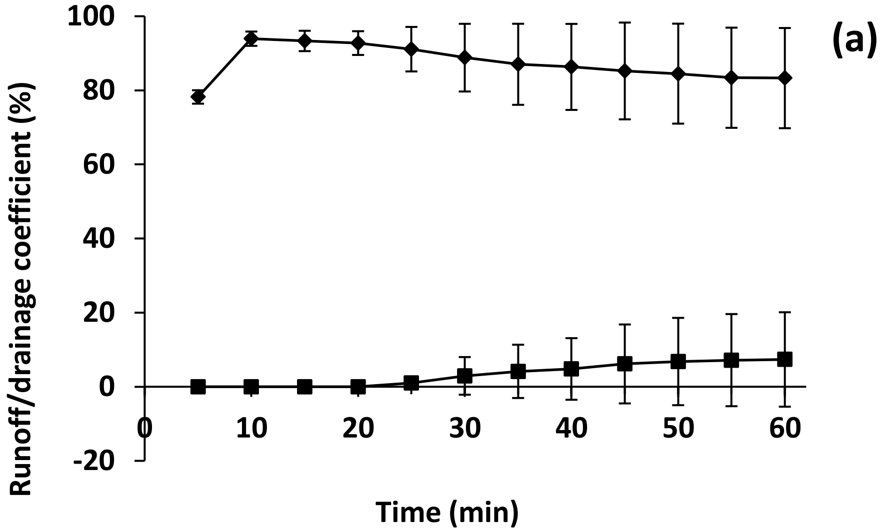

(a)
Runoff/drainage coefficient (%)
100
80
60
40
20
0
-20
0
10
20
30
40
50
60
Time (min)

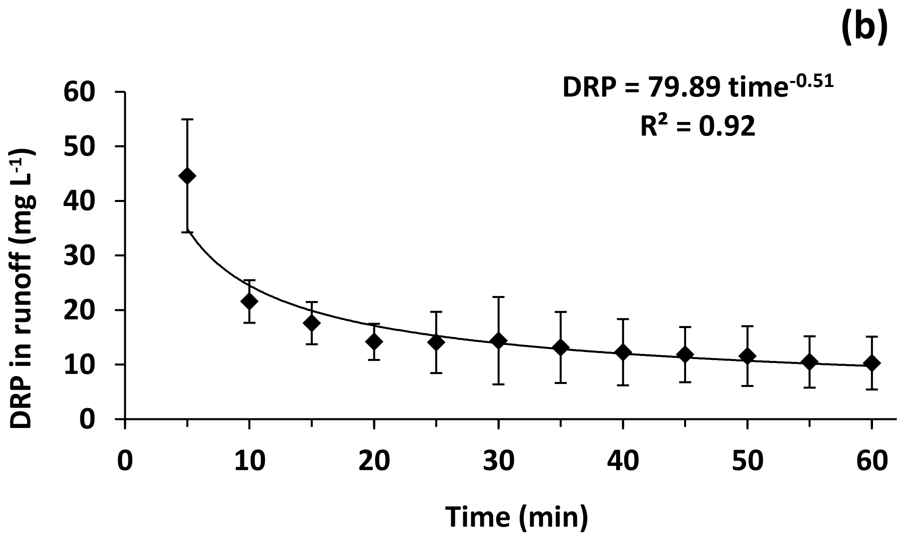

(b)
DRP = 79.89 time$^{-0.51}$
R^2 = 0.92
DRP in runoff (mg L^{-1})
60
50
40
30
20
10
0
0
10
20
30
40
50
60
Time (min)

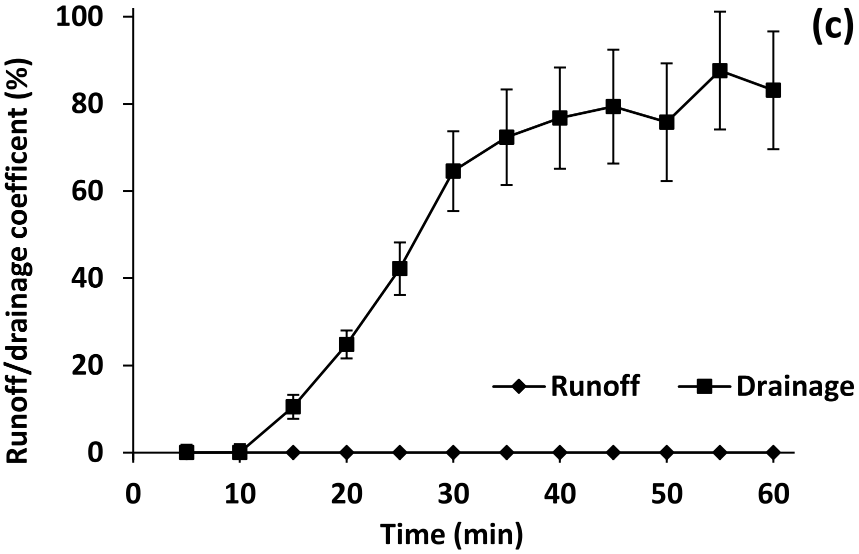
(c)
Runoff/drainage coefficent (%)
100
80
60
40
20
0
0
10
20
30
40
50
60
Time (min)
Runoff
Drainage

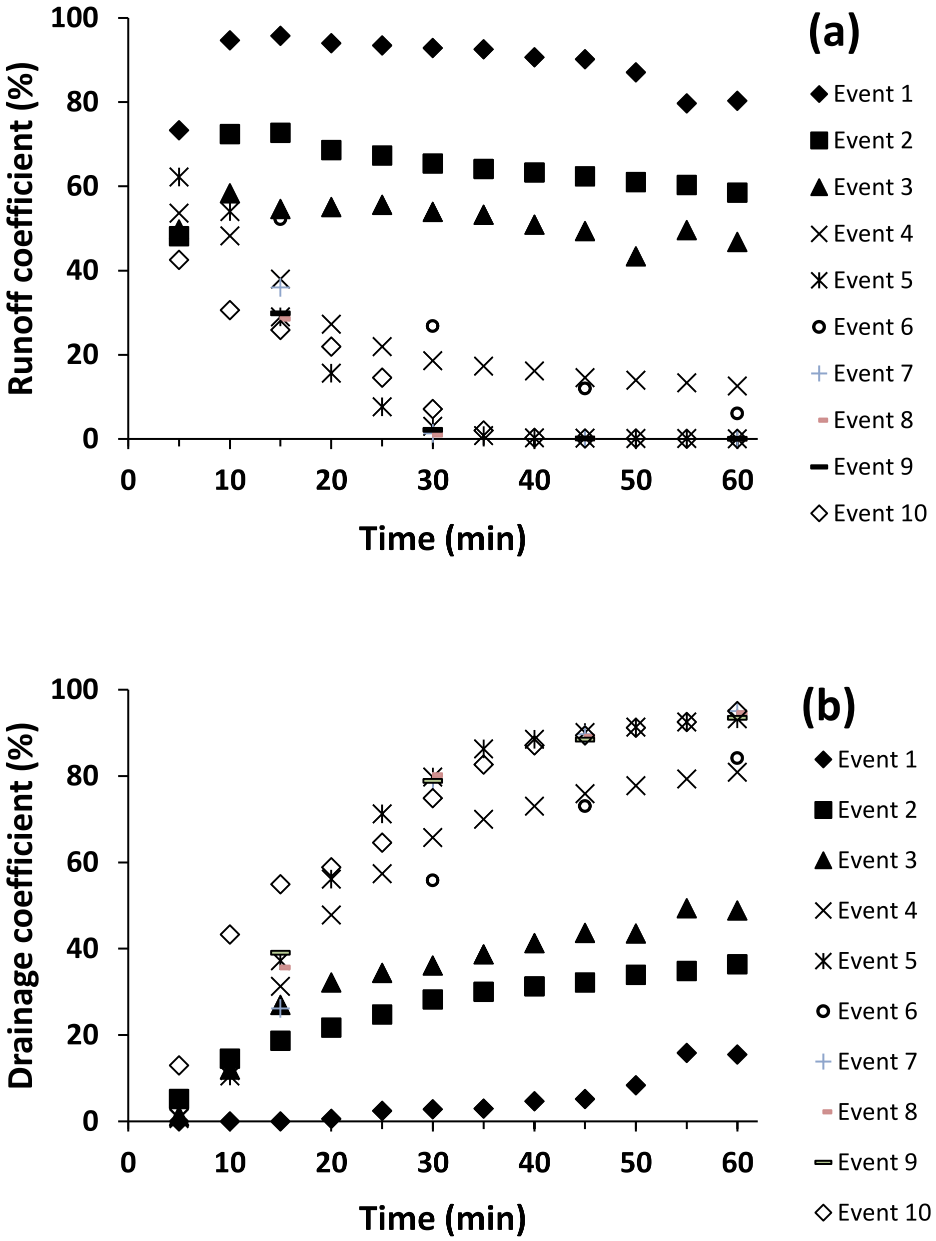
(a)
Runoff coefficient (%)
0
20
40
60
80
100
0
10
20
30
40
50
60
Time (min)
Event 1
Event 2
Event 3
Event 4
Event 5
Event 6
Event 7
Event 8
Event 9
Event 10
(b)
Drainage coefficient (%)
0
20
40
60
80
100
0
10
20
30
40
50
60
Time (min)
Event 1
Event 2
Event 3
Event 4
Event 5
Event 6
Event 7
Event 8
Event 9
Event 10

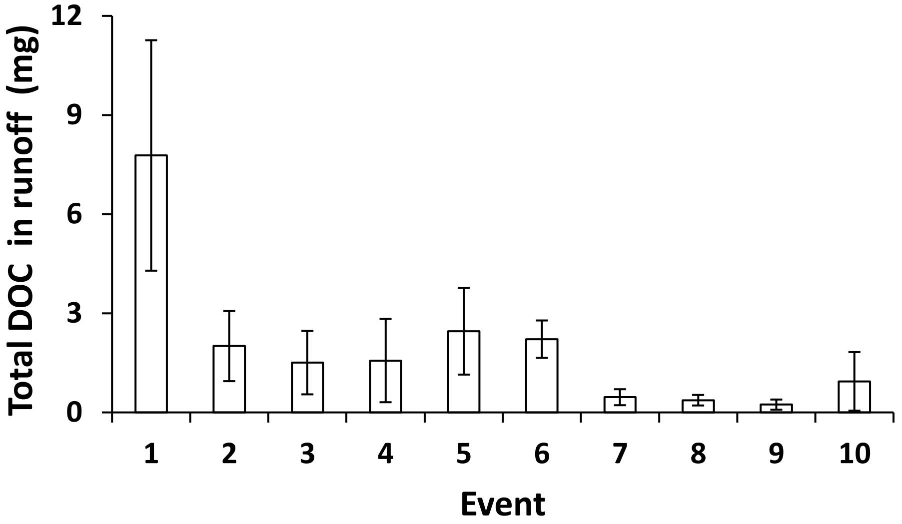
Total DOC in runoff (mg)
12
9
6
3
0
1
2
3
4
5
6
7
8
9
10
Event

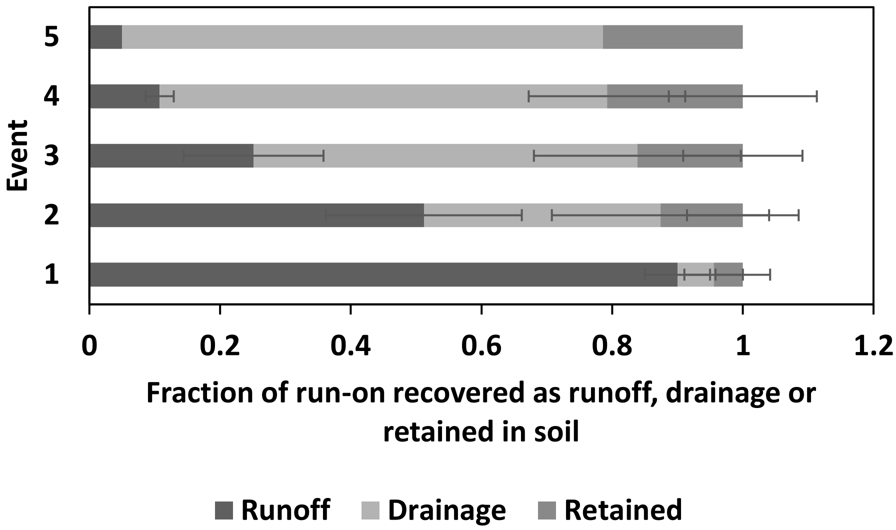
5
4
3
2
1
Event
0
0.2
0.4
0.6
0.8
1
1.2
Fraction of run-on recovered as runoff, drainage or retained in soil
Runoff
Drainage
Retained

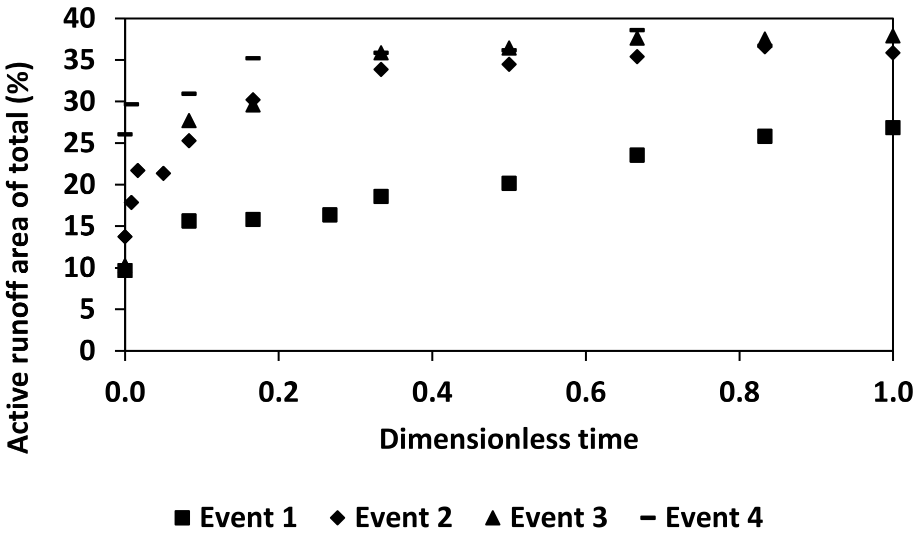
Active runoff area of total (%)
40
35
30
25
20
15
10
5
0
0.0
0.2
0.4
0.6
0.8
1.0
Dimensionless time
Event 1
Event 2
Event 3
Event 4

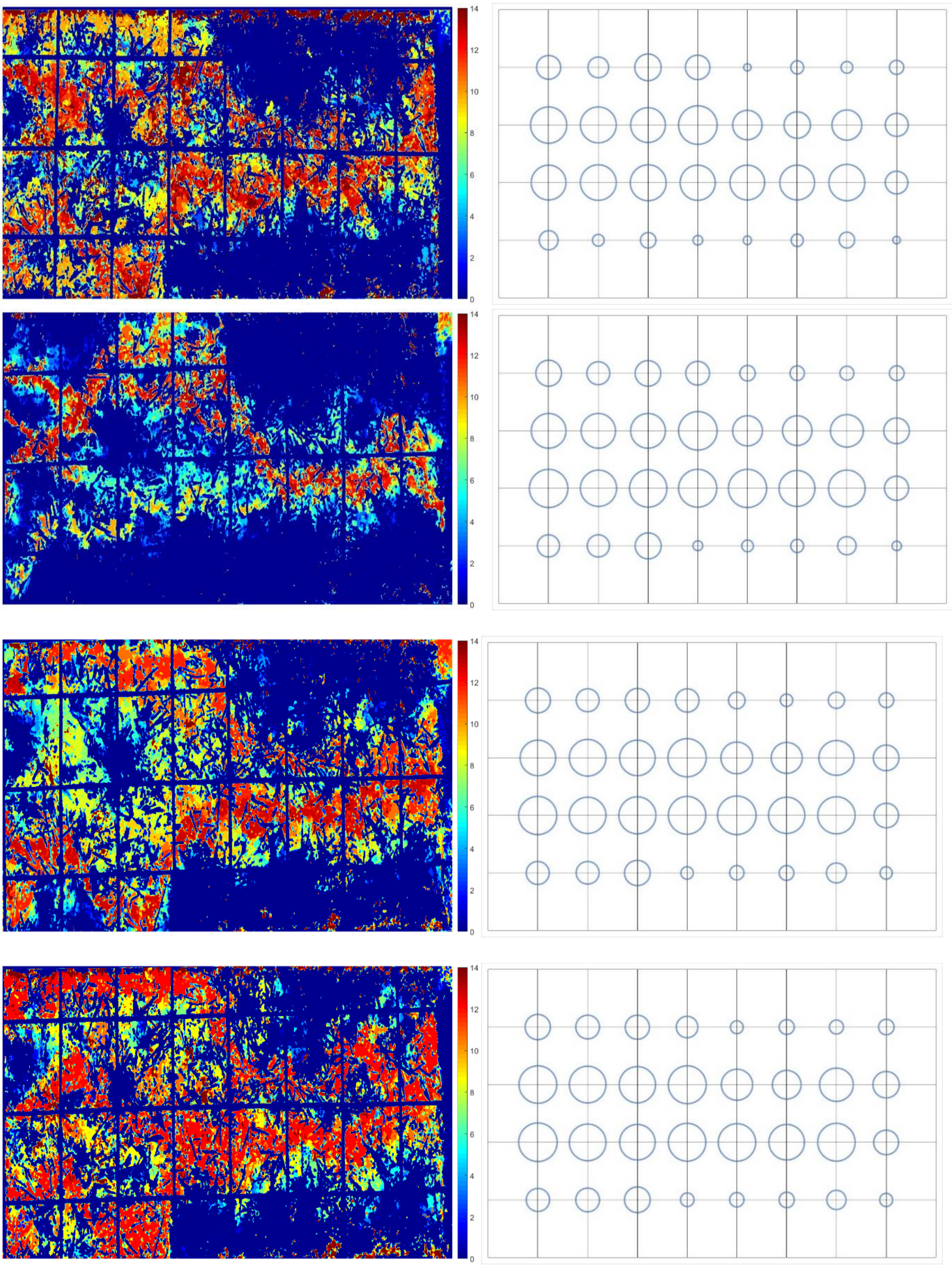
14
12
10
8
6
4
2
0

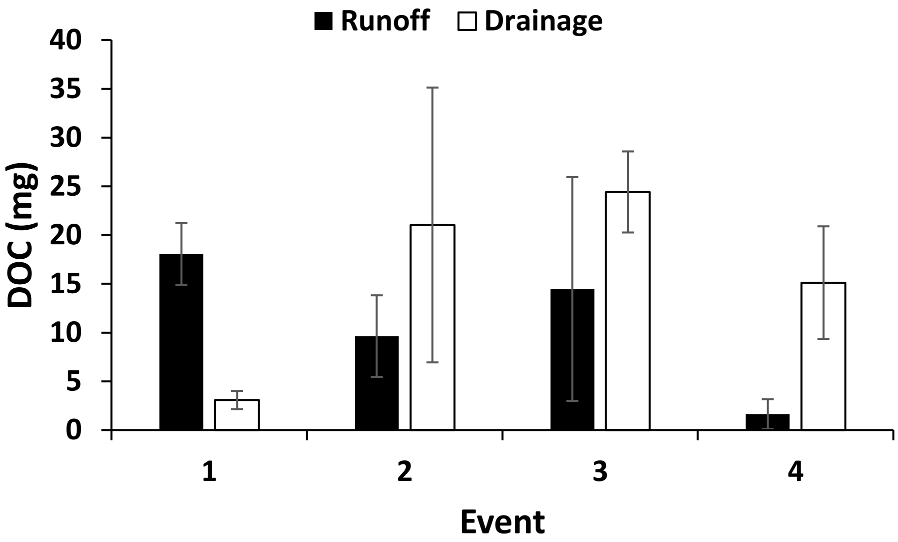
Runoff
Drainage
DOC (mg)
40
35
30
25
20
15
10
5
0
1
2
3
4
Event

References

American Public Health Association, American Water Works Association, Water Environment Federation, 2013. Standard methods for the examination of water and wastewater, 22nd edition.

Arnalds, O., 2008. Andosols. In: W. Chesworth (Ed.), Encyclopedia of Soil Science. Springer, pp. 39-46.

Bezdec, J.C., 1981. Pattern recognition with fuzzy objective function algorithms. Plenum Press, New York.

Blakemore, L., Searle, P.L., Daly, B.K., 1987. Methods for Chemical Analysis of Soils. New Zealand Soil Bureau Scientific Report 80, pp. 103.

Burch, G.J., Moore, I.D., Burns, J., 1989. Soil hydrophobic effects on infiltration and catchment runoff. Hydrological Proceses 3, 211-222.

Cantón, Y., Solé-Benet, A., de Vente, J., Boix-Fayos, C., Calvo-Cases, A., Asensio, C., Puigdefábregas, J., 2011. A review of runoff generation and soil erosion across scales in semiarid south-eastern Spain. Journal of Arid Environments 75(12), 1254-1261.

Contreras, S., Canton, Y., Sole-Benet, A., 2008. Sieving crusts and macrofaunal activity control soil water repellency in semiarid environments: Evidences from SE Spain. Geoderma 145(3-4), 252-258.

Darboux, F., Robin, J.G., Fox, D., 2008. Evaluation of two soil conditioners for limiting post-fire erosion as part of a soil conservation strategy. Soil use and management. 24(4), 366-372.

de Jonge, L.W., Jacobsen, O.H., Moldrup, P., 1999. Soil water repellency: Effects of water content, temperature, and particle size. Soil Sci. Soc. Am. J. 63(3), 437-442.

Dekker, L.W., Doerr, S.H., Oostindie, K., Ziogas, A.K., Ritsema, C.J., 2001. Water repellency and critical soil water content in a dune sand. Soil Sci. Soc. Am. J. 65, 1667-1675.

Dekker, L.W., Jungerius, P.D., 1990. Water repellency in the dunes with special reference to the Netherlands. Catena Supplement 18, 173-183.

Doerr, S., 1998. On standardizing the 'water drop penetration time' and the 'molarity of an ethanol droplet' techniques to classify soil hydrophobicity: a case study using medium textured soils. Earth Surface Processes and Landforms 23, 663-668.

Doerr, S.H., Moody, J.A., 2004. Hydrological effects of soil water repellency: on spatial and temporal uncertainties. Hydrological Processes 18(4), 829-832.

Doerr, S.H., Shakesby, R.A., Walsh, R.P.D., 2000. Soil water repellency: its causes, characteristics and hydro-geomorphological significance. Earth-Science Reviews 51, 33-65.

Fabis, J., Bach, M., Frede, H.G., 1993. Vegetative filter strips in hilly areas of Germany, Proceedings of the International Symposium. American Society of Agricultural Engineers, St. Joseph, Michigan, pp. 81-88.

FAO, 2006. World reference base for soil resources. World Soil Resources Reports No. 103, FAO, Rome.

Ferreira, R.V., Serpa, D., Cerqueira, M.A., Keizer, J.J., 2016. Short-time phosphorus losses by overland flow in burnt pine and eucalypt plantations in north-central Portugal: A study at micro-plot scale. Sci.Total Environ. 551, 631-639.

Flury, M., Flühler, H., 1995. Tracer characteristics of Brilliant Blue FCF. Soil Sci. Soc. Am. J 59, 22-27.

Gee, G.W., Or, D., 2002. Particle size analysis. In: J.H. Dame, G.C. Topp (Eds.), Methods of Soil Analysis – Part 4 – Physical Methods. Soil Science Society of America, Madison, Wisconsin, pp. 255-293.

Ghani, A., Dexter, M., Perrott, K.W., 2003. Hot-water extractable carbon in soils: a sensitive measurement for determining impacts of fertilisation, grazing and cultivation. Soil Biology and Biochemistry 35(9), 1231.

Gomi, T., Sidle, R.C., Miyata, S., Kosugi, K.i., Onda, Y., 2008a. Dynamic runoff connectivity of overland flow on steep forested hillslopes: Scale effects and runoff transfer. Wat. Resourc. Res. 44(8), n/a-n/a.

Gomi, T., Sidle, R.C., Ueno, M., Miyata, S., Kosugi, K.i., 2008b. Characteristics of overland flow generation on steep forested hillslopes of central Japan. Journal of Hydrology 361(3-4), 275-290.

Hart, M.R., Quin, B.F., Nguyen, M.L., 2004. Phosphorus runoff from agricultural land and direct fertilizer effects: A review. J. Environ. Qual. 33(6), 1954-1972.

Horne, D.J., McIntosh, J.C., 2000. Hydrophobic compounds in sands in New Zealand - extraction, characterisation and proposed mechanisms for repellency expression. Journal of Hydrology 231-232, 35-46.

Horton, H.E., 1933. The role of infiltration in the hydrologic cycle. Transactions of the American Geophysical Union 14, 446-460.

Jarvis, N.J., 2007. A review of non-equilibrium water flow and solute transport in soil macropores: principles, controlling factors and consequences for water quality. European Journal of Soil Science 58(3), 523-546.

Jeyakumar, P., Müller, K., Deurer, M., van den Dijssel, C., Mason, K., Le Mire, G., Clothier, B., 2014. A novel approach to quantify the impact of soil water repellency on run-off and solute loss. Geoderma 221-222, 121-130.

Keizer, J.J., Coelho, C.O.A., Shakesby, R.A., Domingues, C.S.P., Malvar, M.C., Perez, I.M.B., Matias, M.J.S., Ferreira, A.J.D., 2005. The role of soil water repellency in overland flow generation in pine and eucalypt forest stands in coastal Portugal. Aust. J. Soil Res. 43(3), 337-349.

Lamparter, A., Bachmann, J., Deurer, M., Woche, S.K., 2010. Applicability of ethanol for measuring intrinsic hydraulic properties of sand with various water repellency levels Vadose Zone J 9, 445-450.

Lascelles, B., Favis-Mortlock, D.T., Parsons, A.J., Guerra, A.J.T., 2000. Spatial and temporal variation in two rainfall simulators: Implications for spatially explicit rainfall simulation experiments. Earth surface processes and landforms 25, 709-721.

Leighton-Boyce, G., Doerr, S.H., Shakesby, R.A., Walsh, R.P.D., 2007. Quantifying the impact of soil water repellency on overland flow generation and erosion: a new approach using rainfall simulation and wetting agent on in situ soil. Hydrological Proceses 21, 2337-2345.

Lowe, D., 2004. Distinctive image features from scale-invariant keypoints. International Journal of Computer Vision 60(2), 91-110.

Miyata, S., Kosugi, K., Nishi, Y., Gomi, T., Sidle, R.C., Mizuyama, T., 2010. Spatial pattern of infiltration rate and its effect on hydrological processes in a small headwater catchment. Hydrological Processes 24, 535-549.

Müller, K., Deurer, M., Jeyakumar, P., Mason, K., van den Dijssel, C., Green, S., Clothier, B., 2014. Temporal dynamics of soil water repellency and its impact on pasture productivity. Agric. Wat. Manage. 143(0), 82-92.

Neff, E.L., 1979. Why rainfall simulation?, Proceedings of the rainfall simulator workshop. USDA Science and Education Administration. Agricultural Reviews and Manuals. ARM-W-10, Tuscon, Arizona, pp. 3-7.

Pierson, F.B., Moffet, C.A., Williams, C.J., Hardegree, S.P., Clark, P.E., 2009. Prescribed-fire effects on rill and interrill runoff and erosion in a mountainous sagebrush landscape. Earth Surface Processes and Landforms 34, 193-203.

Pierson, F.B., Robichaud, P.R., Moffet, C.A., Spaeth, K.E., William, C.J., Hardegree, S.P., Clark, P.E., 2008. Soil water repellency and infiltration in coarse-textured soils of burned and unburned sagebrush ecosystems. Catena 74, 98-108.

Regalado, C.M., Ritter, A., 2005. Characterizing Water Dependent Soil Repellency with Minimal Parameter Requirement. Soil Sci. Soc. Am. J. 69(6), 1955.

Reynolds, W.D., Elrick, D.E., 1991. Determination of hydraulic conductivity using a tension infiltrometer. Soil Sci. Soc. Am. J. 55, 633-639.

Reynolds, W.D., Elrick, D.E., 2005. Measurement and Characterization of Soil Hydraulic Processes. In: J. Álvarez-Benedí, R. Munoz-Carpena (Eds.), Soil-Water-Solute Process Characterization. CRC Press, Boca Raton, pp. 197-252.

Rickson, J., 2002. Experimental techniques for erosion studies: Rainfall simulation, http://www.silsoe.cranfield.ac.uk/staff/cv/rainfall_simulation.pdf.

Ritsema, C.J., 1997. Recurring fingered flow pathways in a water repellent sandy field soil. Hydrology and Earth System Sciences 4, 777-786.

Ritsema, C.J., Dekker, L., Nieber, J., Steenhuis, T.S., 1998. Modeling and field evidence of finger formation and finger recurrence in a water repellent sandy soil. Wat. Resourc. Res. 34(4), 555-567.

Roy, J.L., McGill, W.B., 2002. Assessing soil water repellency using the molarity of ethanol droplet (MED) test. Soil Sci. 167, 83-97.

Ruiz-Sinoga, J.D., Martinez-Murillo, J.F., Gabarron-Galeote, M.A., Garcia-Marin, R., 2010. Effects of exposure, scrub position, and soil surface components on the hydrological response in small plots in southern Spain. Ecohydrology 3(4), 402-412.

Shakesby, R.A., Doerr, S.H., Walsh, R.P.D., 2000. The erosional impact of soil hydrophobicity: current problems and future research directions. Journal of Hydrology 231-232, 178-191.

The MathWorks Inc., 2017. MATLAB and Statistics Toolbox Release 2017a, Natick, Massachusetts, United States.

Tossell, R.W., Wall, G.J., Rudra, R.P., Dickinson, W.T., Groenevelt, P.H., 1990. The Guelph rainfall simulator II: Part 2 - a comparison of natural and simulated rainfall characterstics. Canadian Agricultural Engineering 32(2), 215-223.

Urbanek, E., Walsh, R.P.D., Shakesby, R.A., 2014. Patterns of soil water repellency change with wetting and drying: the influence of cracks, roots and drainage conditions. Hydrological Processes, n/a-n/a.

Valeron, B., Meixner, T., 2010. Overland flow generation in chaparral ecosystems: Temporal and spatial variability. Hydrological Processes 24, 65-75.

Wijewardana, N.S., Müller, K., Moldrup, P., Clothier, B., Komatsu, T., Hiradate, S., de Jonge, L.W., Kawamoto, K., 2016. Soil-water repellency characteristic curves for soil profiles with organic carbon gradients. Geoderma 264, Part A, 150-159.

Zhang, X.C., Norton, L.D., Hickman, M., 1997. Rain pattern and soil moisture content effects on atrazine and metolachlor losses in runoff. J. Environ. Qual. 26, 1539-1547.